Effect of substrate type on the parameters of CdSe-TSC Schottky diode

K. A. Mohammed[a,*], M. M. Hadi[b], A. S. Al-Kabbi[c], K. M. Ziadan[c]
[a]*Department of Medical Physics, Hilla University College, Babylon, Iraq*
[b]*Department of medical Instrumentation Technology Engineering, Hilla University College, Babylon, Iraq*
[c]*Department of Physics, College of Science, Basra University, Basra, Iraq*

CdSe capped with Tri sodium citrate (TSC), nanoparticles were organized by chemical process at ambient conditions. Spin casting technique was used to deposit thin films on substrates from glass at room temperature. Schottky junctions have been fabricated by depositing CdSe thin films using the spin coating on Aluminum (Al) and Florien Tin Oxide (FTO) coated glass substrates and their properties have been investigated by current–voltage measurements. The characteristics obey the pure thermionic emission theory and the contact showed a good rectifying behavior in both structures.

(Received April 17, 2021; Accepted July 16, 2021)

Keywords: CdSe, Schottky, Thin films, Thermionic emission, Spin coating

1. Introduction

The development of nanostructured semiconductor materials over many decades, as well as their possession of unique and distinctive properties, has led to their use in many different applications [1]. Among various semiconductor materials, cadmium selenide (CdSe) is an important direct-band semiconductor with band gap (Eg) pf 1.74 eV, having unique optical properties resulting from quantum confinement effect and wide tuning of bandgap with particle size [1]. This semiconductor has several crystal structures, the first of which is the hexagonal (wurtzite type), which is obtained by high temperature preparation methods, while the other is the cubic structure (zinc-blende type), which is obtained by low temperature preparation methods. The hexagonal state is the stable phase while the sphalerite cubic is the metastable state [2].

Many methods and techniques were used to deposited CdSe thin film like electrodeposition [3] solvothermal [4] chemical bath deposition (CBD) thermal evaporation technique [5].

Though, among these methods, spin coating technique is desirable for the deposition of nanostructured thin films as it is easy to prepare, low cost, and appropriate for large area preparation. Since the properties and efficiency of materials are enhanced when employed in their nanocrystalline forms, research interest has grown immensely in areas of obtaining CdSe in their Nano particulate sizes. One of the recent trends in nanomaterials research is the control of particle shape, by manipulating the precursor concentration, temperature of reaction, and capping environment, which are factors that affect the morphology and size of the nanoparticles [6]. excellent photoelectrical characteristics and make it a promising material for applications in many fields, such as photo detectors, FETs, field emitters, solar cells, LEDs, memory devices, biosensors, and biomedical imaging [7].

Schottky barrier diodes (SBD) are of the most simple of metal–semiconductor (MS) contact devices. have been studied extensively due to their technological importance in microelectronic devices [8].

Measurements of current–voltage (I–V) of Schottky barrier give information about the conduction process and the nature of barrier formation at the MS interface.

The aim of this present work is to prepare and fabricate schottky cadmium selenide thin films by a simple spin coating process on glass, florane tin oxide (FTO) coated glass and Aluminum substrates diodes to study the effect of substrate type on the parameters of schottky diodes.

[*] Corresponding author: kahtan444@gmail.com
https://doi.org/10.15251/CL.2021.187.421

2. Experimental details

2.1. CdSe Nanoparticles Preparation

CdSe Nanoparticles were prepared and characterized according to our papers[9][10]

2.2. Fabrication of the devices.

A thin film schottky diodes with the structure Glass/FTO/CdSe-TSC/Ag and Al/CdSe-TSC/Ag have been fabricated in which CdSe layer was deposited on top of the FTO coated glass substrate and Al substrate

3. Results and discussions

The size and morphology of CdSe nanoparticles have been examined by scanning electron microscopy, transmission electron microscopy (TEM) and atomic force microscopy(AFM). The image of the CdSe NPs. From TEM test showing in Fig. 1, display spherical mono dispersed particles of 20-90 nm with an average diameter about 44 nm. It is clear from FESEM and AFM images that the thin film surface is smooth and has spherically shaped grains. The surface is covered with uniformly size grains. No cracks or holes are observed in the thin films .The mean grain sizes of films were about 40 nm.

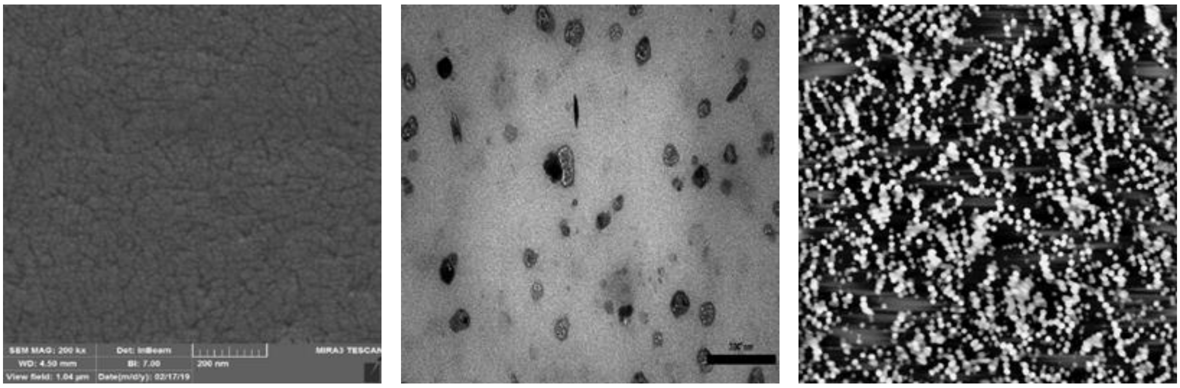

a) *b)* *c)*

Fig. 1. TEM micrograph (a) FESEM micrograph (b) AFM micrograph (c) of CdSe NPs. Capped with TSC.

The X-ray diffract gram for thin film of CdSe capping with TSC is shown in Fig. 6. The peaks obtained in the Figure has been compared with the typical configuration of the cubic structure of CdSe (J.CPDS 19-0191). The forms of XRD point toward that the film of CdSe consist of particles in nano-scale [16]. The peak intensity at 2θ=25.46 which is corresponding with the planes (111) is higher than the other peaks, which confirms the growth of thin films along this plane. There are no detection of peaks resultant from impurities that suggestion the great purity of produced matter. The intensity of the peaks is quite an indication of the well crystalline nature of the prepared nanoparticles.

The average grain size (G) of the crystalline material which outplays a significant turn in the material properties by Full Width of Half Maximum (FWHM) method can be estimated simply from the X-ray spectrum. Williamson-hall plot is a well-known equation for relating the crystallite size to the growing [11]

$$\beta\cos\theta = \frac{k\lambda}{G} + 4\varepsilon\sin\theta \qquad (1)$$

where G is the crystallite size (nm), k is a constant (0.94 for spherical particles), λ is the wavelength of the x-ray radiation (Cu-Kα = 0.1541 nm), β is the full width at half maximum (FWHM) of the intense and broad peaks and θ is the Bragg's or diffraction angle.

Where G was equal to 2.68 nm .It is slightly larger than we got from the Sherar r- Debay relationship, which was roughly 1.78 [9]

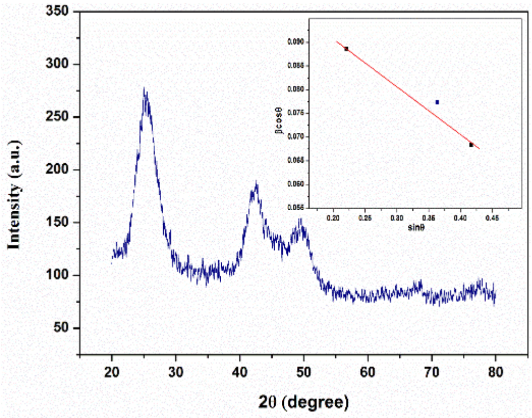

Fig. 2. X-ray diffraction pattern of CdSe NPs. Capped with TSC and the inset figure represent the plot of Williamson-Hall.

UV-VIS absorption spectra for CdSe nanoparticles shown in Fig. 5, The range of the absorption edge lies between 650 nm to 420 nm, which is a pronounced blue shift from 712 nm of the bulk CdSe[12], indicating that particles in nanoscale[13].

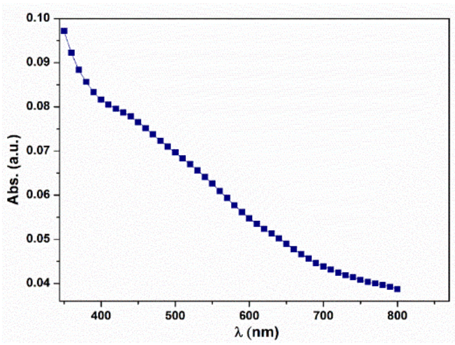

Fig. 3. Absorption spectra of CdSe nanoparticles capped with TSC.

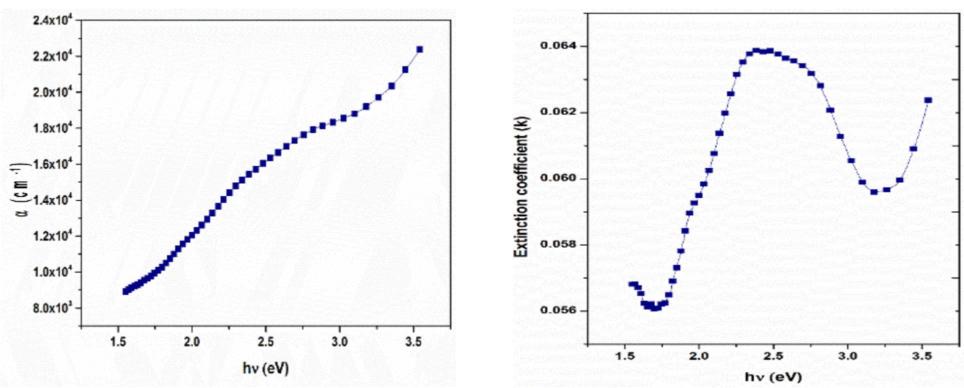

Fig. 4. Absorption and extinction coefficient of CdSe nanoparticles capped with TSC.

Fig. 5 shows the plot of (αhυ)2 vs. hυ for CdSe-TSC thin film. From the plot of the figure, the value of Eg is found to be 2.25 which is more as compared to bulk CdSe (1.7 eV) due to quantum confinement effect.

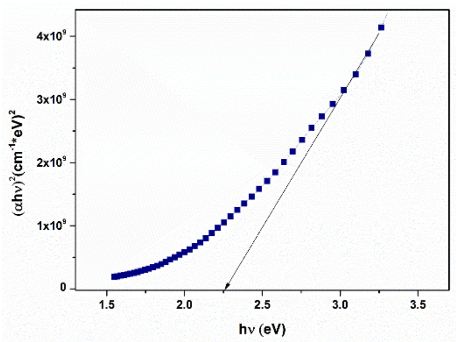

Fig. 5. The energy band gap of CdSe nanoparticles capped with TSC.

Photoluminescence (PL) is a very public emission spectroscopy characterization method for studying the properties of nanomaterials since it is simple and direct[14] Fig. 6 show the Photoluminescence emission spectra of CdSe nanoparticles at the different excitation wavelength. It is clear from the figure that the emission peaks of all three excitation wavelength nearby the green, at 548 nm. From PL peak, The band gap of CdSe nanoparticle are founded equal to2.13eV. There is a blue shift compared with the bulk CdSe (720 nm) because of the quantum confinement effect[15].

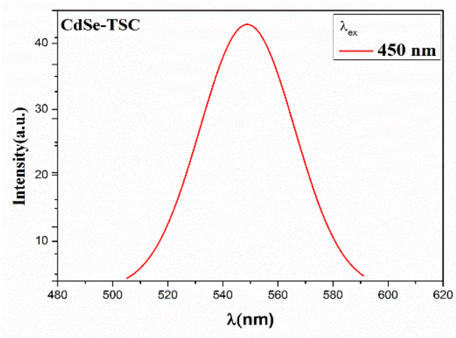

Fig. 6. Photoluminescence spectrum of CdSe-TSC, at excitation wavelength equal to 450 nm.

AL/CdSe-TSC/Ag and FTO/CdSe-TSC/Ag Schottky diodes have been fabricated and measured in dark at room temprature . These were studied using Keithley 2400, under forward and reverse bias voltages -5 to +5 V aroomtemperature, where the electrical measurements have performed fabricated by sandwich configuration. The diodes show nonlinear and rectifying I-V characteristics, establishing the proper configuration of the junction.

In AL/CdSe-TSC/Ag the reverse current was observed to be very weak and the forward current increased sharply with the bias voltage. In addition, the photocurrent exponentially increases with the increase in the forward bias voltage where its behavior was found to be nonlinear. both the films showed good rectifying nature.

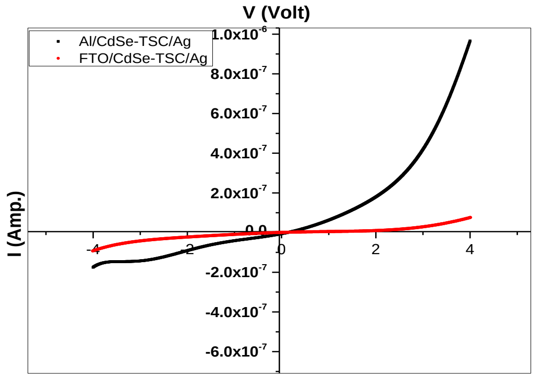

Fig. 7. The current–voltage (I–V) characteristics of Al/CdSe-TSC/Ag and FTO/CdSe-TSC/Ag Schottky diodes.

To investigate the electron transport in this hybrid thin-film based device, the fitted I-V curves are shown in To further understand the electric-field-induced transition, we have tried to fit the I -V characteristics for the two diodes with theoretical models. The plot of log*(I)* versus log*(V)* is shown in Fig. 8 a.

I-V plots for the diodes fit the space charge limited conduction (SCLC) mechanism. The plot fits to a straight line, showing the validity of the SCLC mechanism for the FTO/CdSe-TSC/Ag diode [16]. We find that the characteristics of the Al/CdSe-TSC/Ag can be fitted to an injection-dominated mechanism where I-V fitted with I-$V^{1/2}$. showing the validity of the thermionic emission model [17]. From this results we can conclude that the type of substrate can change the conduction mechanism of CdSe. The linear behavior of log(I) –log(V) plot shows the presence of space-charge-limited current (SCLC) mechanism through the junction. Its observed that the double logarithmic plot of forward bias I– V Characteristics for Al/CdSe- TSC/Ag have two linear regions. The region (I) have slope of 2.2, while the region (II) has the slope of 1.72. The decreases in slope at high voltage could be due to 'trap-filled' limit of the device at high voltage [18].

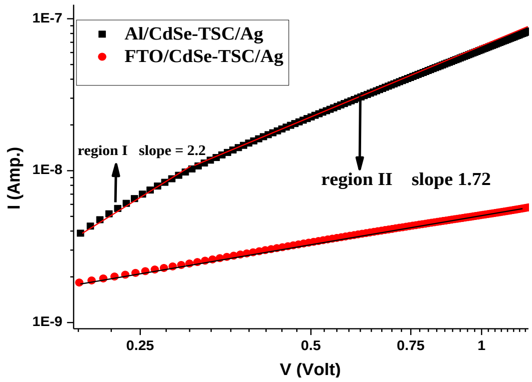

Fig. 8. a The current–voltage log(I)-log(v) of Al/CdSe-TSC/Ag and FTO/CdSe-TSC/Ag schottky diodes.

According to the SBD theory, the relationship between current and voltage is given by [19]

$$I = I_0 \exp\left(\frac{qV}{nkT}\right) \tag{2}$$

$$I_0 = AA^{**}T^2 \exp[-q\Phi_{B0}/kT] \tag{3}$$

where A is the diode area, A∗ is the effective Richardson constant, k is Boltzmann constant, T is the temperature, Φ_{B0} is the barrier height and q is the electron charge. n is a measure of conformity of the diode to pure thermionic emission and it is determined from the slope of the straight line region of the forward bias ln J -V characteristics through the relation:

$$\eta = \frac{q}{kT}\frac{\mathrm{d}V}{\mathrm{d}\ln J} \tag{4}$$

Ideality factor was equal to 10.2 and 14.1 for Al/CdSe-TSC/Ag and FTO/CdSe-TSC/Ag respectively.

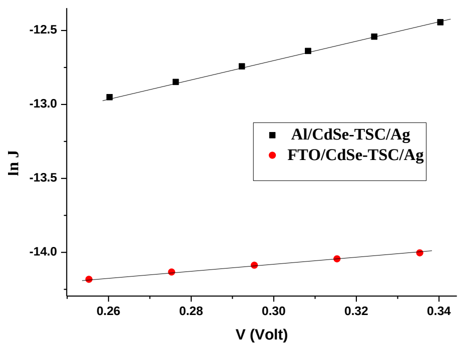

Fig. 8 b. The current–voltage ln(J)- ln (v) of Al/CdSe-TSC/Ag and FTO/CdSe-TSC/Ag schottky diodes.

4. Conclusion

From the obtained results of the present work, we conclude the following: TEM and FESEM AFM micrograph of CdSe NPs. Capped with TSC images indicate that the thin film surface is smooth and has spherically shaped grains. The surface is covered with uniformly size grains. . particles of 20-90 nm with an average diameter about 44 nm.
XRD analysis confirmed that CdSe NPs. Capped with TSC nanoparticles prepared in this research are well crystalline nature of the prepared nanoparticles. The UV-VIS absorption spectra for CdSe nanoparticles shown .The range of the absorption edge lies between 650 nm to 420 nm, which is a pronounced blue shift from 712 nm of the bulk CdSe indicating that particles in nanoscale.

The band gap of CdSe nanoparticle are founded equal to2.13eV. There is a blue shift compared with the bulk CdSe (720 nm) because of the quantum confinement effect. Show the Photoluminescence emission spectra of CdSe nanoparticles at the different excitation wavelength. It is clear from the figure that the emission peaks of all three excitation wavelength nearby the green, at 548 nm. From PL peak. The electrical measurements have performed fabricated by sandwich configuration. The diodes show nonlinear and rectifying I-V characteristics, establishing the proper configuration of the junction.

In AL/CdSe-TSC/Ag the reverse current was observed to be very weak and the forward current increased sharply with the bias voltage. We find that the characteristics of the Al/CdSe-TSC/Ag can be fitted to an injection-dominated mechanism where I-V fitted with I-$V^{1/2}$, showing the validity. The decreases in slope at high voltage could be due to 'trap-filled' limit of the device at high voltage. Ideality factor was equal to 10.2 and 14.1 for Al/CdSe-TSC/Ag and FTO/CdSe-TSC/Ag respectively.

References

[1] Dhar, Rakesh, Suman Singh, Atul Kumar, Bulletin of Materials Science **38**(5), 1247 (2015).
[2] Phukan Pallabi, Dulen Saikia, International Journal of Photoenergy, 2013.
[3] Mahato Somnath, Asit Kumar Kar, Journal of Science: Advanced Materials and Devices **2**(2),

165 (2017).
[4] S. Suresh, C. Arunseshan, Applied Nanoscience **4**(2), 179 (2014).
[5] Rodríguez-Rosales, K., Nieto-Zepeda, K., Quiñones-Galván, J. G., Santos-Cruz, J., Mayén-Hernández, S. A., Guillen-Cervantes, A., De Moure-Flores, F., Chalcogenide Letters, 17(10), 529-536. (2020).
[6] Damian C. Onwudiwe, Madalina Hrubaru, Eno E. Ebenso, Journal of Nanomaterials, 2015.
[7] Lijuan Zhao, Linfeng Hu, Xiaosheng Fang, Advanced Functional Materials **22**(8), 1551 (2012).
[8] S. S. Patel, B. H. Patel, T. S. Patel, Journal of Experimental and Industrial Crystallography **43**(5), 542 (2008).
[9] Kahtan A.Mohammed, Alaa S. Al-Kabbi, Kareema M. Zidan, AIP Conference Proceedings **2144**(1), 2019.
[10] Kahtan A.Mohammed, Alaa S. Al-Kabbi, Kareema M. Ziadan, IOP Conference Series: Materials Science and Engineering **757**(1), 2020.
[11] S. Mustapha et al., Advances in Natural Sciences: Nanoscience and Nanotechnology **10**(4), 045013 (2019).
[12] Duck Jong Suh et al., Korean Journal of Chemical Engineering **19**(3), 529 (2002).
[13] G. Ramalingam, J. Madhavan, Investigation on the structural and morphological behavior of CdSe nanoparticles by hydrothermal method, **3**(3), 217 (2011).
[14] Kumar, Challa SSR, ed. UV-VIS and photoluminescence spectroscopy for nanomaterials Characterization, Berlin: Springer, 2013.
[15] N. G. Semaltianos et al., EPL (Europhysics Letters) **84**(4), 47001 (2008).
[16] K. Mohanta, S. K. Majee, S. K. Batabyal, A. J. Pal, Journal of Physical Chemistry B **110**(37), 18231 (2006).
[17] B. C. Das, A. J. Pal, Philosophical Transactions of the Royal Society A: Mathematical, Physical and Engineering Sciences **367**(1905), 4181 (2009).
[18] R. K. Gupta, K. Ghosh, P. K. Kahol, Current Applied Physics **9**(5), 933 (2009).
[19] Güllü, Ömer, Abdulmecit Türüt, Materials Science-Poland **33**(3), 593 (2015).